Mon. Not. R. Astron. Soc. **000**, 1–6 (2005) Printed 5 February 2008 (MN LATEX style file v2.2)

Constraints on the dense matter EOS from the measurements of PSR J0737-3039A moment of inertia and PSR J0751+1807 mass

M. Bejger⋆, T. Bulik† and P.Haensel‡
Nicolaus Copernicus Astronomical Center, Bartycka 18, 00716 Warsaw, Poland

Accepted .... Received ....; in original form .....

ABSTRACT
The moment of inertia of the pulsar A in the neutron star binary J0737-3039 will soon be measurable through detailed measurements of the periastron advance. We present the calculation of the moment of inertia of neutron stars with the masses of the components of the binary J0737-3039 for a broad range of equations of state of dense matter and discuss the implications of such measurement for constraining the equation of state. An observational determination of the moment of inertia of the pulsar A in J0737-3039 with the accuracy of 10% shall narrow down considerably the range of viable equations of state. We also show that limits on maximal mass of a neutron star provide a complementary set of constraints on the properties of dense nuclear matter.

Key words: stars:neutron - equation of state - binaries: pulsars

1 INTRODUCTION

Constraining the equation of state (EOS) of dense matter in the interior of neutron stars is a fundamental problem of modern astrophysics. At present, many different theoretical EOSs at densities exceeding nuclear density ($\rho_0 = 2.5 \times 10^{14}$ g cm^{-3}) are available. Their predictions diverge at a few times ρ_0, which reflects poor knowledge of the EOS of neutron star cores. To constrain the EOS, one needs to measure neutron star masses and radii or some functions of these quantities. This is an extremely difficult task.

Neutron star masses are best known for the radio pulsars residing in binaries. The estimates of their masses have been achieved by measuring the post-Keplerian parameters of binary motion. The best studied cases are the double neutron star binaries, like e.g. the Hulse-Taylor pulsar, or the recently discovered binary pulsars J0737-3039A,B (Burgay et al. 2003). Masses have also been strongly constrained in some binaries with white dwarfs (Nice et al. 2004a,b). Masses of the accreting neutron stars have been constrained by measuring the motion and spectral properties of the companions. The latter, however, suffer from larger systematic uncertainties because of difficulty in modeling atmospheres of stars illuminated by X and gamma rays from the neutron star.

⋆ E-mail:bejger@camk.edu.pl
† E-mail:bulik@camk.edu.pl
‡ E-mail:haensel@camk.edu.pl

Constraining a second parameter like e.g. radius or any function of the mass and radius is much more difficult. One can achieve that by measuring the thermal UV or soft X-ray radiation from the surface of a neutron star (Pavlov & Zavlin 2003). The estimates of the radius depends in this case on precise modeling of the spectrum in the presence of strong magnetic field and with unknown chemical composition of the atmosphere. The constraints on the radius depend also on the estimate of the distance to the source. Identification of spectral lines in the soft X-ray spectra would provide an estimate of the gravitational redshift of a neutron star. However, no such line have been reliably identified yet (results of Cottam et al. 2002 still need a confirmation). The discovery of kHz QPOs raised hopes to constrain masses and radii of neutron stars. These oscillations are most likely connected with motion in the inner disk around a neutron star. The estimates based on the QPO frequencies depend on a particular model of the QPO phenomena and also are uncertain due to erratic behavior of the oscillations.

The discovery of the binary pulsars J0737-3039A,B provided an opportunity to test General Relativity and pulsar physics in a unprecedented detail. The system is highly relativistic, and only a few months of observations led to the constraints similar to those of the Hulse-Taylor system after a decade (Lyne et al. 2004). It is a nearly edge on binary which provides an opportunity to investigate the region inside the light cone of pulsar B. The measurements of the pulsar motion are precise enough to measure the second or-

der post-Newtonian (2PN) effects. At this level of accuracy the periastron advance depends also on the spin-orbit coupling which involves the moment of inertia of pulsar A. The possibility of using this effect to measure a neutron star moment of inertia was first noted by Damour & Schaefer (1988). Lattimer & Schutz (2004) estimated that the moment of inertia of pulsar A should be measurable with the accuracy of about 10%. Morrison et al. (2004) presented a calculation of the moment of inertia for three classes of equations of state and showed that such measurement would allow to distinguish between these classes.

The moment of inertia of a neutron star is a very interesting quantity as it involves the square of the radius. Therefore, for a given mass, it is very sensitive to the details of the EOS, and in particular its stiffness. Sensitivity of $I(M)$ to the EOS was already utilized in the analyses of the energetics of the Crab Nebula expansion, powered by the Crab Pulsar at the expense of the neutron star rotation energy. Resulting values of I were rather high, indicating a stiff EOS (Bejger & Haensel 2002, 2003). This result is in accordance with very recent measurements of the mass of the PSR J0751+1807, which at the 95% confidence level is $2.1^{+0.4}_{-0.5}$ $M_\odot$ (Nice et al. 2004a).

In the case of PSR J0737-3039 A the gravitational mass is already very precisely known (1.338 $M_\odot$) and perspectives of the future measuring of I_A via analysis of the effect of the spin-orbit coupling in the pulsar timing motivate a detailed calculation of the moment of inertia. Here we use a broad set of EOSs in order to study various correlations involving the type of the EOS and I_A, and discussing observational constrains from measurements of stellar moment of inertia and mass. In section 2 we briefly describe the EOSs we use, and we present the method of calculating the moment of inertia. Section 3 contains the results, while in section 4 we present the summary and discussion.

2 CALCULATING MOMENTS OF INERTIA

2.1 Description of EOSs

To illustrate the broad range of possible values of the moment of inertia, we use a set of twenty three EOSs of dense matter available in the literature. Similarly as Morrison et al. (2004), we divide the EOSs into three classes. The first class contains EOSs involving only nucleons and leptons, based on realistic nuclear interactions fitted to nuclear-physics data, and obtained using modern, precise solutions of the many-body problem (**Class I** : APR of Akmal et al. 1998, WFF1-3 of Wiringa et al. 1988, BBB1-2 of Baldo et al. 1997, SLy of Douchin & Haensel 2001, FPS of Pandharipande & Ravenhall 1989). Out of these EOSs, only FPS and APR models were considered by Morrison et al. (2005). We added two EOSs based on the Brueckner-Bethe-Goldstone theory of nuclear matter (BBB1, BBB2), one EOS derived from the Skyrme effective nucleon-nucleon interaction, consistent with variational calculations for dense neutron matter (SLy), and three EOSs (WFF1-3) obtained in variational calculations of Wiringa et al. (1988).

A second class contains EOS with less solid nuclear and many-body basis, but allowing for more speculative extrapolations : non-relativistic effective forces and relativistic mean-field models involving nucleons and hyperons, and models with phase transitions to kaon condensates and quark matter (**Class II**: GNH1-4 of Glendenning 1985, WGW1-2C of Weber et al. 1991, BGN1H2, BGN2H1, BGN2H2 of Balberg & Gal 1997; Balberg et al. 1999, GNHQ of Glendenning 1997 (mixed-phase hadron-quark EOS, model 2) and PREPL of Pons et al. 2000). This set of EOSs is much larger and richer than Class II of Morrison et al. (2005), who restricted themselves to two EOSs obtained using the Relativistic Mean Field model.

Finally, third class is the most exotic, as it includes models of self-bound strange (quark) stars (**Class III**: DBDRS of Dey et al. 1998 and SM, SM60 of Zdunik 2000). This class contains only three EOSs because the scaling relation (see Sect.3) enables one to easily predict results for any EOS of strange quark matter intermediate between the stiffest SM60 EOS and the softest DBDRS EOS.

Moreover, we considered additionally three specific EOSs of extremal character. Two of them are stiff (MFT17, Haensel et al. 1981) and soft (BPAL12, Bombaci 1995) extremes of the nucleonic EOSs; they set two boundaries for the baryonic EOSs. While they reproduce experimental saturation density, binding energy, and symmetry energy of nuclear matter, they strongly overestimate (MFT17) or underestimate (BPAL12) nuclear matter incompressibility at saturation. We also consider the CLES EOS that does not belong to any of above classes I-III. The causal-limit (CLES) EOS maximizes the maximum allowable stellar mass. This EOS assumes the SLy EOS below density $2\rho_0 = 5\times10^{14}$ g cm^{-3} and the stiffest possible (sound speed equal the speed of light) EOS at higher density.

2.2 Numerical technique

The moment of inertia of a neutron star is calculated assuming rigid rotation, and in general case it is defined as J/Ω, where J is the stellar angular momentum and Ω is the angular frequency of rigid rotation as measured by a distant observer. If Ω is much smaller than the mass-shedding (Keplerian) limit for a given mass, $\Omega_{\rm ms}$, then a slow rotation approximation is valid, and I can be calculated using non-rotating stellar model (Hartle 1967). In the case of J0737-3039 A pulsar $\Omega = 276.8{\rm s}^{-1}$ is less than one tenth of $\Omega_{\rm ms}$, and therefore the Hartle approximation should be valid within a percent (corrections to it are $\propto (\Omega/\Omega_{\rm ms})^2$).

The values of moments of inertia for hydrostatic stellar models based on the presented EOSs were obtained while solving the Tolman-Oppenheimer-Volkoff equation (Tolman 1939; Oppenheimer & Volkoff 1939) for spherically symmetric star, within the slow-rotation approximation (Hartle 1967). Additionally, for a representative subset of EOS we have directly checked the accuracy of this approximation by computing the moment of inertia for the axisymmetric rotating stellar model within the highly accurate 2-D LORENE framework (Bonazzola et al. 1993, 1998). The virial error indicators which describe the accuracy of computation were typically 10^{-5} or less. As one could suspect, the difference between non-rotating and axisymmetric rotating models at this rotation rate is of the order of $\sim$ 1% or less. It is principally dominated by the difference in methods of interpolating the tabulated EOS. Therefore, we draw the conclusion that the spherically symmetric calculations are per-

Table 1. Highly accurate 2-D results for rotating axisymmetric stellar models of gravitational mass $M = 1.338\ M_\odot$ and rotational frequency $\Omega = 276.79\ \mathrm{s}^{-1}$ computed using the LORENE subroutines for a small subset of EOSs. The symbol $\rho_{\mathrm{c},14}$ denotes the central density (in units of $10^{14}\ \mathrm{g\,cm}^{-3}$), J_{47} [$10^{47}\ \mathrm{cm}^2\,\mathrm{g\,s}^{-1}$] - the angular momentum, $I_{45} = J/\Omega$ [$10^{45}\ \mathrm{g\,cm}^2$] the moment of inertia and R_{circ} the circumferential radius (in km). In general, the values of the moment of inertia differ by approximately 1% from the non-rotating results - the difference is dominated by the error of the tabulated EOS interpolation method.

EOS	$\rho_{\mathrm{c},14}$	J_{47}	I_{45}	R_{circ}
BPAL12	19.57	2.72	0.98	10.52
APR	9.74	3.39	1.23	11.35
SLy	9.39	3.57	1.29	11.76
BGN2H1	6.09	4.53	1.64	13.47
GNH3	6.18	4.77	1.72	14.28

fectly suitable for reasonable estimation of the moment of inertia for J0737-3039 components. The results for the slow-rotation approximation for both pulsar components of the J0737-3039 system are displayed in Fig. 1, and the precise parameters for a small subset of EOSs (for pulsar A) are collected in Table 1.

3 RESULTS

The dependence of the predicted values of I_{A} and I_{B} on the assumed EOS of dense matter is visualized in Fig. 1. Within the considered set of EOSs $I_{\mathrm{A},45} = 0.7 - 1.9$ and $I_{\mathrm{B},45} = 0.7 - 1.7$, a huge scatter indeed (we adopt the notation $I_{45} \equiv I/10^{45}$ g cm^2). However, if we restrict ourselves to most recent EOSs consistent with experimental nuclear matter parameters and involving only nucleons, then the range of predicted values narrows considerably, to $I_{\mathrm{A},45} = 1.1 - 1.3$ and $I_{\mathrm{B},45} = 1.0 - 1.2$. The EOSs which involve hyperons and/or exotic phases of dense matter (quark and kaon condensate) at supra-nuclear densities turn out to be so stiff for neutron stars with the masses of the pulsars A and B that they yield $I_{\mathrm{A},45} = 1.4 - 1.7$ and $I_{\mathrm{B},45} = 1.3 - 1.6$. Their high stiffness within PSR J0737-3039A,B results from the requirement that they should produce maximum allowable mass $> 1.44\ \mathrm{M}_\odot$. The maximum mass is sensitive to the high-density segment of the EOS, with strong softening due to hyperons or a phase transition. For this segment to be sufficiently stiff to respect consistency with observations, the lower-density segment (without hyperons and/or new dense phase) should be indeed very stiff. The two extremes of nucleon EOSs set are MFT17 (very stiff) and BPAL12 (very soft); while they reproduce experimental saturation density, binding energy, and symmetry energy of nuclear matter, they strongly overestimate (MFT17) or underestimate (BPAL12) nuclear matter incompressibility.

The values obtained for the causal-limit CLES EOS (open star symbols) are similar to those obtained for the Class II EOSs. At relatively low neutron star masses, the SLy envelope with $\rho < 2\rho_0$ is important for stars structure. However, the core with $v_{\mathrm{sound}} = c$ shifts up the values of

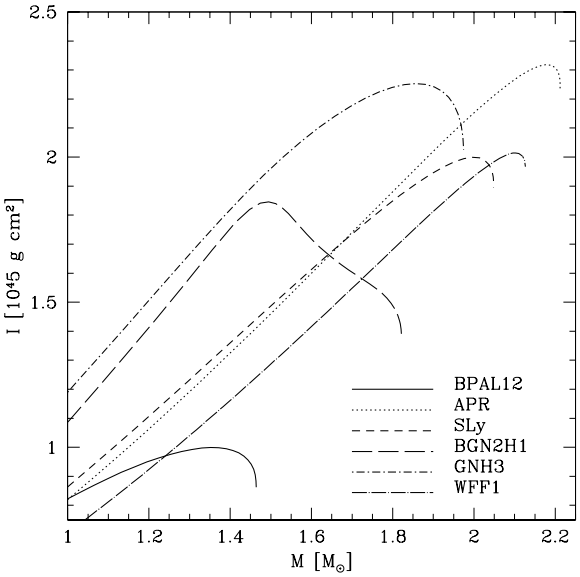

Figure 2. The dependence of the moment of inertia on the gravitational mass for a few representative equations of state.

$I_{\mathrm{A,B}}$, by more than twenty percent, compared to the SLy ones.

A separate subset of EOSs (open triangles) is composed of three models of self-bound strange quark matter. The values of $I_{\mathrm{A},45}$ and $I_{\mathrm{B},45}$ predicted by the strange-star models are very scattered $0.7-1.7$. However, this range of values can be easily understood in terms of the scaling properties of I and M with the value of the surface density of strange stars. To a very good approximation the values of I_{A} and I_{B} calculated for different EOSs of strange quark matter are related by a simple relation involving surface density of bare strange stars (= density at zero pressure), ρ_{s}. Namely, I_{A} calculated for the EOS with zero pressure density ρ_{s} is related to I'_{A}, calculated for the EOS with ρ'_{s}, by $I'_{\mathrm{A}} \simeq (\rho_{\mathrm{s}}/\rho'_{\mathrm{s}})^{2/3} I_{\mathrm{A}}$ (this relation is obtained using constant-density Newtonian star models). Therefore, huge disparity in I_{A} for the DBDRS and SM60 EOS can be accounted for by the difference in ρ_{s}. We considered bare strange-star models of J0737-3039 A, B. However, the mass of the crust of strange stars is at most $10^{-4}\ M_\odot$, and therefore its contribution to I is at most 0.01% and can be safely neglected.

4 SUMMARY AND DISCUSSION

We have presented the moments of inertia of neutron stars J0737-3039 A, B for 25 different EOSs of dense matter. Inspection of Fig. 1 leads to conclusion that a measurement of I_{A} with a 10% precision would necessarily imply rather precise picking up of the EOS of matter in J0737-3039 A. It could be a stringent test of "realistic EOSs" of Class I. Either the EOS inside J0737-3039 A is stiffer than our best nuclear models predict and belongs to Class II, or is in harmony with nuclear many-body theory represented at its best by Class I. We therefore confirm and extend the result of Morrison et al. (2004). While it would be difficult to eliminate strange star model altogether, measurement of I_{A}

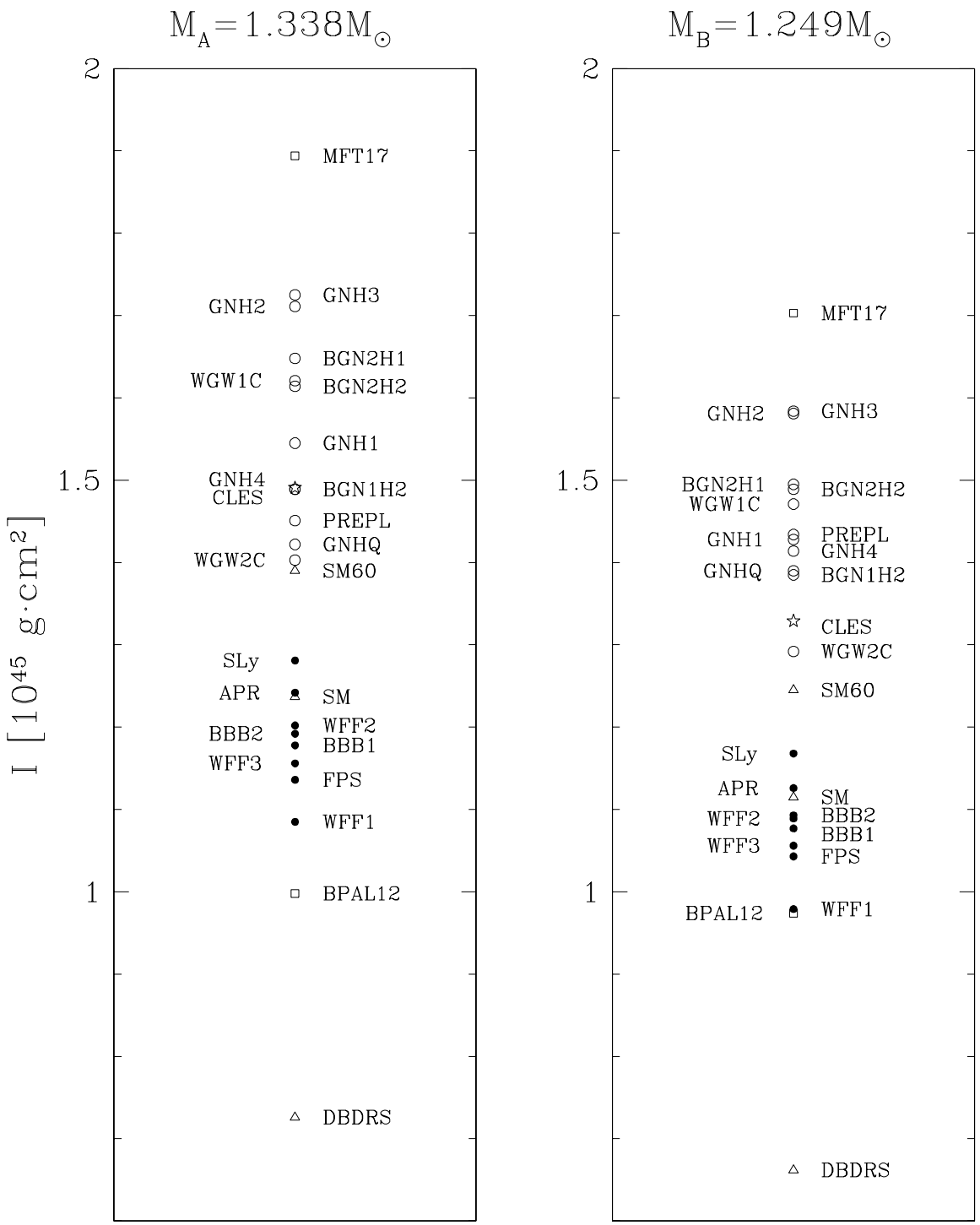

Figure 1. The moments of inertia of the binary pulsar components: A- left panel, and B - right panel. Filled circles: Class I (realistic EOSs involving nucleons and leptons). Open circles: Class II (relativistic and non-relativistic mean-field models involving hyperons, kaon condensates and quark matter). Open triangles: Class III - strange quark stars; the range of values of the moment of inertia available for strange stars lies between the triangles labeled DBDRS and SM60. Open squares: extreme nucleonic EOS. Open star: causal-limit EOS (CLES). For further explanations see the text.

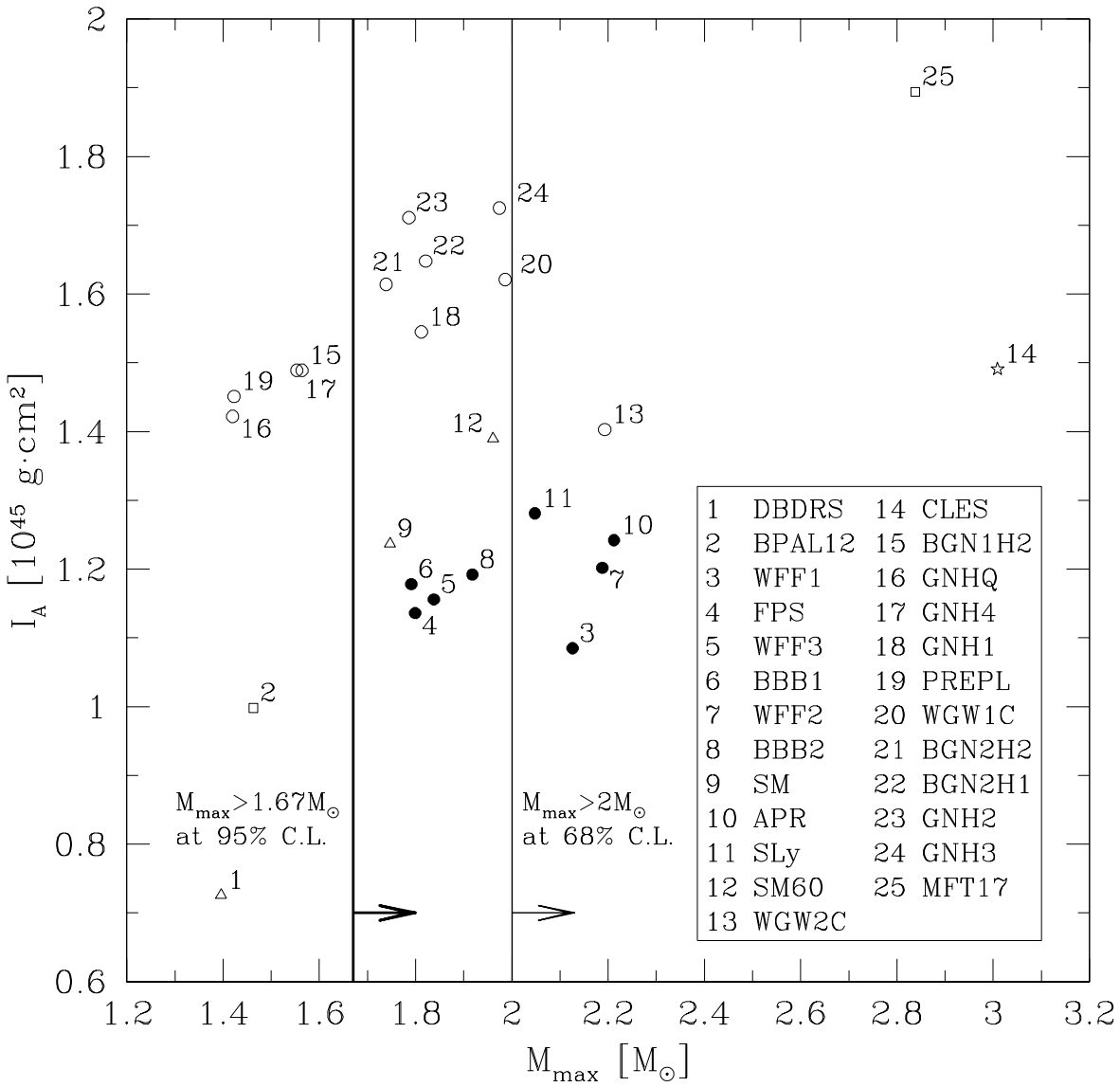

Figure 3. Moment of inertia of a neutron star with mass of pulsar A versus the maximum mass of a neutron star plotted for the same set of EOSs as in Fig. 1. The vertical thin solid line denote the 68% confidence lower limit on the maximum mass (2.0 $M_\odot$), whereas the thick solid line marks the 95% confidence limit (1.67 $M_\odot$) - the limits were obtained from the PSR J0751+1807 mass measurements (see text for details).

would strongly limit the value of ρ_s of strange quark matter at zero pressure. The measurement of the moment of inertia I_A will be sensitive to the properties of the EOS for the densities typically in the range of the central density of the pulsar A. From Table 1 we see that this corresponds $\rho < (6-10) \times 10^{14} \mathrm{g\,cm^{-3}}$, i.e. or $\rho < (2-4) \times \rho_0$ where ρ_0 is the nuclear density (see Sect. 1). In this estimate of the density we have neglected the unrealistically soft BPAL12 model.

It should be stressed that hopefully stringent constraints on I_A do not probe the EOS at densities crucial for the value of maximum allowable mass for neutron stars, M_{max}. A good example of two EOSs which yield very similar values for I_A and I_B but very different stars at M_{max} are BPAL12 and WFF1 (Fig. 2). However, as Fig. 3 shows, existence of 2.1 $M_\odot < M_{max}$ neutron star (Nice et al. 2004a) combined with determination, within 10%, of I_A, would quite precisely establish the complete EOS of dense matter inside neutron stars. Lower limits on the maximum mass of a neutron star are sensitive to the properties of the EOS at the density $\rho \approx (6-10) \times \rho_0$, much larger than densities relevant for the constraints from measuring I_A. Both constraints together would constitute an ultimate test of the many-body theories of dense matter.

While the measurement of the moment of inertia of the pulsar A in the J0737 system is approaching it is interest-

ing to speculate about further investigations of the neutron star equation of state. Measuring the moment of inertia of the pulsar B in this system does not look feasible with the current instruments. However precise monitoring with the next generation instruments like e.g. the Square Kilometer Array may yield highly accurate data that enable determination of $I_{\rm B}$, or moments of inertia of neutron stars in other binary pulsar systems. The Parkes Multibeam Survey may also bring discoveries of other highly relativistic binary pulsars, and provide measurements of the moment of inertia of neutron stars with other masses. One should note recent measurements of masses in neutron star white dwarf binaries which hint at the existence of neutron stars with masses as large as $2.1\,M_\odot$ (Nice et al. 2004a,b). Such measurements provide lower limits on the maximum mass of a neutron star and thus are complementary to the measurements of the moment of inertia. Limits on the neutron star maximum mass probe the densest segment of the EOS. We illustrate the strength of the constraints coming from the measurement of the moment of inertia of pulsar A in J0737-3039 system together with limits on the maximum neutron star mass in Fig. 3. The two values - $I_{\rm A}$ and $M_{\rm max}$ are not correlated since they probe different ranges of densities of the EOS. A simultaneous measurement of the moment of inertia of pulsar A with accuracy of $\approx$ 10% with a limit on the maximum mass of neutron star approaching $2.0\,M_\odot$ should narrow down the possible set of nuclear matter EOS to just a few possibilities in the near future. We also plot the lower limits on the maximum mass of a neutron star implied by the recent measurement of the mass of the pulsar PSR J0751+1807 (Nice et al. 2004a). We have obtained the limits shown in the Figure by assuming that the errors on the mass are approximately gaussian. We have then integrated the approximate probability and obtained the 68% lower limit on the maximum mass of 2.0 $M_\odot$, and the 95% limit of 1.67 $M_\odot$. These values are plotted as vertical lines in Fig. 3. Thus a simultaneous measurement of the moment of inertia of pulsar A with accuracy of $\approx$ 10% with a limit on the maximum mass of neutron star approaching $2.0\,M_\odot$ shall narrow down the possible set of nuclear matter EOS to just a few possibilities in the near future.

ACKNOWLEDGMENTS

This work was supported by the following KBN grants 2 P03D 001 25 (TB) and 1 P03D 008 27 (PH and MB).

REFERENCES

Akmal A., Pandharipande V. R., Ravenhall D. G., 1998, Phys. Rev. C, 58, 1804
Balberg S., Gal A., 1997, Nucl. Phys., A625, 435
Balberg S., Lichtenstadt I., Cook G. B., 1999, ApJS, 121, 515
Baldo M., Bombaci I., Burgio G. F., 1997, A&A, 328, 274
Bejger M., Haensel P., 2002, A&A, 396, 917
Bejger M., Haensel P., 2003, A&A, 405, 747
Bombaci I., 1995, in Perspectives on Theoretical Nuclear Physics, ed. I. Bombaci, A. Bonaccorso, A. Fabrocini pp 229–237
Bonazzola S., Gorgoulhon E., Salgado M., Marck J. A., 1993, A&A, 278, 421
Bonazzola S., Gourgoulhon E., Marck J. A., 1998, Phys. Rev. D, 58, 104020
Burgay M., D'Amico N., Possenti A., Manchester R. N., Lyne A. G., Joshi B. C., McLaughlin M. A., Kramer M., Sarkissian J. M., Camilo F., Kalogera V., Kim C., Lorimer D. R., 2003, Nature, 426, 531
Cottam J., Paerels F., Mendez M., 2002, Nature, 420, 51
Damour T., Schaefer G., 1988, Nuovo Cimento, 101, 127
Dey M., Bombaci I., Dey J., Ray S., Samanta B. C., 1998, Phys. Lett., B438, 123
Douchin F., Haensel P., 2001, A&A, 380, 151
Glendenning N., 1997, Nuclear and particle physics of compact stars. Berlin: Springer
Glendenning N. K., 1985, ApJ, 293, 470
Haensel P., Proszynski M., Kutschera M., 1981, A&A, 102, 299
Hartle J. B., 1967, ApJ, 150, 1005
Lattimer J. M., Schutz B. F., 2004, astro-ph/0411470
Lyne A. G., Burgay M., Kramer M., Possenti A., Manchester R. N., Camilo F., McLaughlin M. A., Lorimer D. R., D'Amico N., Joshi B. C., Reynolds J., Freire P. C. C., 2004, Science, 303, 1153
Morrison I. A., Baumgarte T. W., Shapiro S. L., Pandharipande V. R., 2004, ApJ Lett, 617, L135
Nice D. J., Splaver E. M., Stairs I. H., 2004a, ASP Conference Series, F.A. Rasio and I.H. Stairs, astro-ph/0411207
Nice D. J., Splaver E. M., Stairs I. H., 2004b, in IAU Symposium Heavy Neutron Stars? A Status Report on Arecibo Timing of Four Pulsar - White Dwarf Systems. p. 49
Oppenheimer R. C., Volkoff G. M., 1939, Phys. Rev., 55, 374
Pandharipande V. R., Ravenhall D. G., 1989, in NATO ASIB Proc. 205: Nuclear Matter and Heavy Ion Collisions Hot Nuclear Matter. pp 103–132
Pavlov G. G., Zavlin V. E., 2003, in Texas in Tuscany. XXI Symposium on Relativistic Astrophysics Thermal radiation from cooling neutron stars. pp 319–328
Pons et al. J. A., 2000, C62, 035803
Tolman R. C., 1939, Phys. Rev., 55, 364
Weber F., Glendenning N. K., Weigel M. K., 1991, ApJ, 373, 579
Wiringa R. B., Fiks V., Fabrocini A., 1988, Phys. Rev., C38, 1010
Zdunik J. L., 2000, A&A, 359, 311